Effect of a Contraction on Turbulence. Part I: Experiment*

Yong O. Han† William K. George ‡ Johan Hjärne §

Measurements are reported of grid-generated turbulence subjected to a $11.3:1$ **contraction. Three different upstream positions of the grid relative to the contraction were used. Particular effort was made to remove the effect of background disturbances on the measurements. This was especially important for the streamwise fluctuations which decrease through the contraction (due to negative production) while background disturbances are strongly amplified by it.**

The corrected measurements were used to compute the budget of the turbulence kinetic energy, both in the contraction and in the duct preceding it. Over most of the contraction, the energy balance is almost entirely between convection of turbulence energy by the mean flow and the energy production terms. Since, however, the contraction promotes a trend toward isotropy initially, then away from it, there is not only a point at which the kinetic energy is a minimum, but also a nearby *crossing point* where the production terms are identically zero. Hence over a small region, the leading terms in the energy balance are nearly zero. The theoretical implications of these experimental results are considered in Part 2.

Nomenclature

h	Distance into contraction measured from exit, m.
I	Time integral scale, s.

*This is a revised and extended version of AIAA paper 2005 - 1119. January, 2005.

†Professor, Yeungnam University, Gyongsan 712-749, Korea, Member, AIAA. Email: yohan@yu.ac.kr

‡Professor, Department of Applied Mechanics, Chalmers University of Technology, Gothenburg, SE 412 96, Sweden, Member, AIAA. E-mail: wkgeorge@chalmers.se

§Graduate Assistant, Department of Applied Mechanics, Chalmers University of Technology, Gothenburg, SE 412 96, Sweden. Email: hjarne@chalmers.se

f	Frequency, Hz.
f_k	Frequency corresponding to convection of Kolmogorov microscale, Hz.
F_{11}^1	Spectrum of u-velocity component in streamwise direction as function of k_1, m^3/s^2
F_{22}^1	Spectrum of v-velocity component in streamwise direction as function of k_1, m^3/s^2
k	Kinetic energy of turbulence per unit mass, m^2/s^2.
k_1	Wavenumber in streamwise direction computed from $k_1 = 2\pi f/U$, m^{-1}.
M	Mesh size of grid, m.
r	Radial coordinate, m
S	Mean strain rate, s^{-1}.
$S_u(f)$	Frequency spectrum of streamwise velocity component, m^2/s^3.
$S_v(f)$	Frequency spectrum of radial velocity component, m^2/s^3.
T	Record length and averaging time. s.
U, u	Mean and fluctuating streamwise velocities, m/s.
U_o	Mean streamwise velocity at the grid, m/s.
$u^{(n)}$	Contamination velocity from background, m/s.
$u^{(1t)}, u^{(2t)}$	Turbulence velocities at two widely separated points, m/s.
U_o	Mean velocity at grid, 2.00 m/s in experiment, m/s.
V, v	Mean and fluctuating radial velocities, m/s
V_c	Contraction volume as function of distance from exit
x	Streamwise coordinate, m.
η_K	Kolmogorov microscale, $(\nu^3/\epsilon)^{1/4}$, m
ν	Kinematic viscosity , m^2/s.
ϵ	Rate of dissipation of turbulence energy per unit mass, m^2/s^3.

I. Introduction

The flow through a contraction has a special place in the study of turbulence. Such flows are often used to reduce turbulence levels in experimental facilities, as well as to modify turbulence. Examples of the latter include attempts to improve the isotropy of grid-generated turbulence by a slight contraction, and to study how turbulence evolves from one state to another when subjected to an externally imposed strain rate. The energy balance of grid-generated turbulence in a duct with a following contraction is of considerable interest in its own right. This is because the production terms which are generally considered negligible in the duct become increasingly important through the contraction and eventually dominate the energy balance there.

The early studies on turbulence through a contraction were initiated by researchers who were primarily interested in wind tunnel design. In the 1950's, Ribner and Tucker[1] and

Uberoi[2] carried out comprehensive spectral and moment measurements in several contractions with different exit/inlet area ratios. Ramjee and Hussain[3] and Tan-atichat[4] reported extensive measurements with various grids and contractions. These data should have been, and for the most part were, useful for the development of turbulence models. Shabbir,[5] however, carried out a careful analysis of the various experiments using the kinetic energy equation and discovered that all of the high contraction ratio data could be explained *only if the dissipation rates were negative through part of the contraction.* This is clearly a physical impossibility! Shabbir was unable to resolve whether the experiments were themselves incorrect, or whether the calculation of the dissipation by ignoring the turbulence transport terms in the energy balance (a customary assumption in such flows) was wrong. The most recent experiment was by Sjöberg and Johansson[6] who carried out extensive experiments using a grid near the entrance of the 9:1 contraction of a large windtunnel. They were able to make extensive measurements of turbulence quantities including the dissipation, and even infer the pressure-strain rate correlations. In spite of the large contraction ratio, however, the results were of limited value to those interested in rapid distortion theories due to the relatively low ratio of time scales ($Sk/\epsilon < 6$) .

The study reported herein was designed to obtain both a high contraction ratio (11.3:1) and high values of the time scale ratio ($Sk/\epsilon > 50$). All terms in the energy balance believed to be significant were measured or inferred from direct measurement, including the dissipation itself. The experimental measurements were made along the centerline of an axisymmetric flow facility in which isotropic grid turbulence was generated in a duct. The turbulence first decays, then is accelerated through a contraction. By varying the distance of the grid upstream of the duct it was possible to vary both the turbulence intensity entering the contraction, and its spatial scale.

In the following sections, the facility and experimental techniques described, with particular attention to the manner in which background disturbances were accounted for. Finally the data will be presented, and discussed in the context of the Reynolds stress equations appropriate to the flow.

II. The experiment

The wind tunnel constructed especially for these experiments is shown schematically in Figure 1. It consists of a flow-conditioning unit with several fine mesh screens, a duct-like test section, and a contraction. The contraction inlet diameter was 487 mm and the outlet diameter was 145 mm corresponding to an area ratio of 11.3 : 1. The contraction length was 0.62 m, and was followed by a straight section of length 457 mm which exhausted into a large room as a jet. The contraction was originally of matched cubic design, following Morel,[7] but

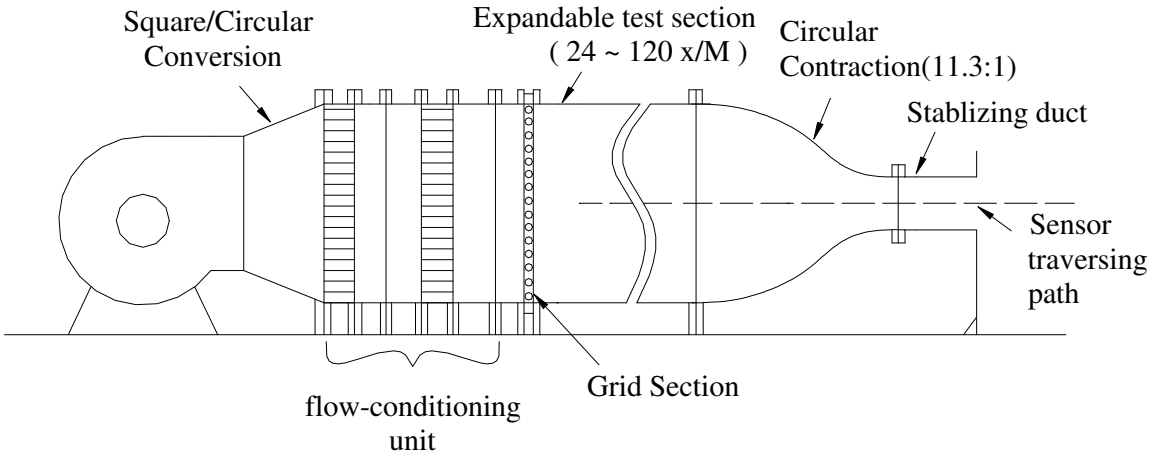

Figure 1. Wind tunnel apparatus showing grid and contraction.

it had been significantly modified before this experiment to adjust it to another facility. The actual contraction shape was measured by sealing off the exit, turning it vertically so the exit was down, then incrementally filling it with water and carefully measuring the water depth, h, as a function of the volume of water added, $V(h)$. These data were then fitted with a fifteenth order polynomial from which the radius as a function of height, $r(h)$, could be computed from the relation $r(h) = \sqrt{(1/\pi)dV_c/dh}$. The actual shape obtained in several ways is shown in Figure 2.

All experiments were conducted with a test section velocity at the grid, $U_o = 2$ m/s. The corresponding exit velocity from the contraction is 21.7 m/s. The turbulence generator was located near the upstream end of the test section. It consisted of a biplane square mesh grid constructed from 6.35 mm diameter circular rods, and assembled with a mesh size of $M = 0.0254$ m (44% solidity). The grid Reynolds number was approximately $3,400$ for all experiments described below. The test section was comprised of several separable sections which could be rearranged (or removed entirely) to adjust the grid position up to a maximum distance of 3.05 m (or 120 mesh lengths) upstream of the contraction. For the contraction experiments, the grid was placed at four different positions ahead of the contraction inlet plane: 0.61 m, 1.12 m, 1.73 m and 3.05 m, which are denoted as $24M$, $44M$, $68M$ and $120M$ respectively. The latter was useful for characterizing the behavior of the grid, but the turbulence intensities were too low for reliable measurement in the contraction. Note that the conditions upstream of the grid remained constant for all experiments.

Figure 3(left) shows the variation of the centerline mean velocity with streamwise distance through the duct and contraction. Figure 3(right) shows that the slight but increasing mean

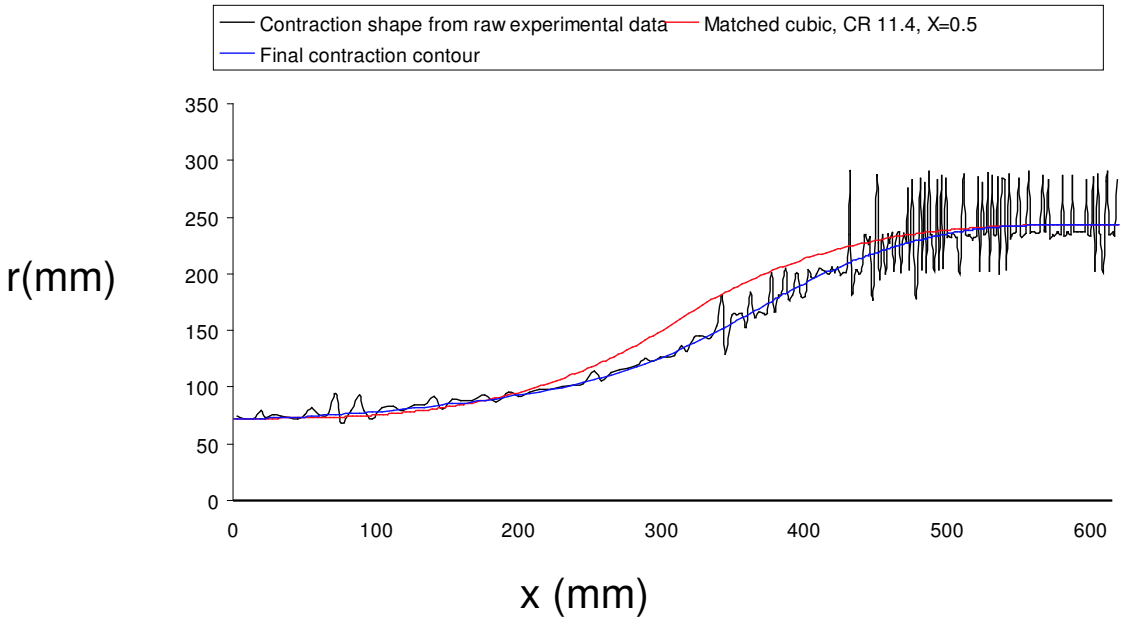

Figure 2. Contraction shape.

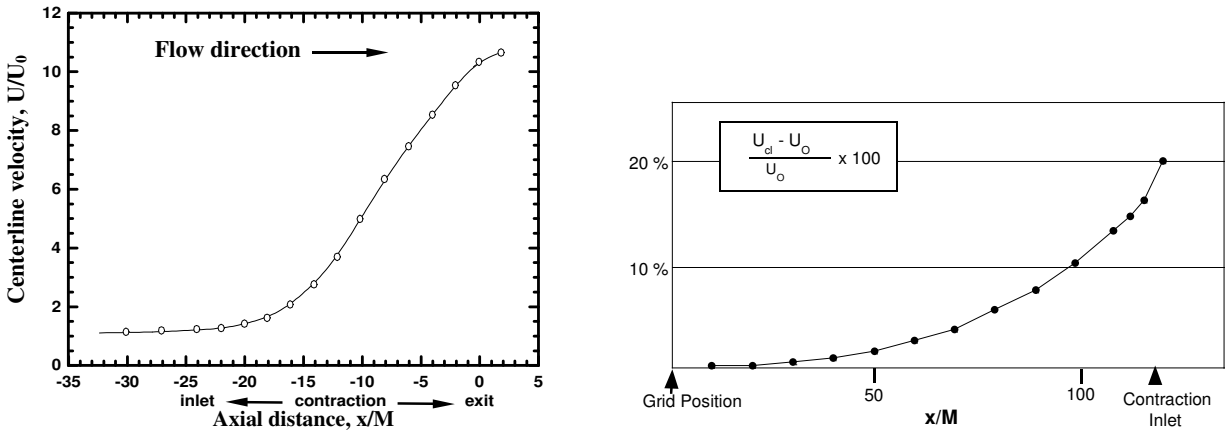

Figure 3. left: Centerline mean velocity through the contraction ($M = 0.0254$ m, $U_o = 2$ m/s). right: $100(U_{cl} - U_o)/U_o$ showing upstream acceleration in percent as function of distance from grid (grid at x/M=120).

velocity acceleration begins well upstream of the contraction. Similar effects were noted by Han[8] using longer contractions as well. The acceleration is due in part to the growth of the boundary layers on the wall, but also in part a consequence of inviscid flow theory. The streamlines upstream (or downstream) of a contraction (or diffuser) can be parallel only at infinity, a fact ignored by the usual simplistic streamtube analysis in which it is *assumed* that $U \cdot A = constant$. Whichever its cause, this slight acceleration of the flow in the duct played a role in the *apparent* decay rate of the turbulence downstream of the grid

and upstream of the contraction by creating a slightly faster rate of decay of $\langle u^2 \rangle$ than for $\langle v^2 \rangle$ due to the small streamwise production of turbulence energy (see analysis in Part 2). The difference between the actual flow and the streamtube analysis is even more important in the contraction where the streamline curvature is most significant. Initially the inward curving streamlines correspond to an increasing pressure with radius, so the potential flow slows down with increasing radius (since $p/\rho + U^2/2 = constant$) and the velocity profile is non-uniform (although still axially symmetric). The opposite happens when the streamline curvature reverses near the exit, with a consequence that the minimum velocity is now at the centerline.

III. Instrumentation for turbulence measurements

Flow velocities were measured by both single hot-wires and x-wires. The probes were constructed from 5μm diameter copper-plated tungsten wires which were welded onto Dantec 55P01 and 55P51 probe bodies. The wires were then etched leaving a sensitive area of approximately 3 mm, which was less than twice the Kolmogorov microscale length, η_K, for all experimental conditions. This permitted direct measurement of the velocity time derivatives by minimizing the spatial filtering. The spatial separation between wires in the x-wire probes was less than 2 mm. The CTA's were Dantec 55M's with 55M10 bridges, and were operated at the highest possible gain setting consistent with their stability (Gain = 6). The overheat ratio was set at 0.6 to minimize sensitivity to room temperature fluctuations while maximizing probe life. The calibration of the hot-wires utilized a digital linearizing scheme, and the angle calibration of the x-wires was carried out by tilting the wires and fitting a modified cosine law.

The anemometer outputs were low-pass filtered using Dantec 55D26 signal conditioning units ($-$12dB/oct) set at about twice the highest frequency corresponding to the convected Kolmogorov microscale ($f_k = U/\eta_K$). Because this frequency varies as the local flow velocity through the contraction, values of the low-pass cutoff ranged from 200 Hz to 1.3 kHz depending on position. In order to directly measure the dissipation, the time derivative of the velocity signals was obtained by using the +6dB high-pass filters provided in the Dantec 55D26 signal conditioners. From linear systems theory it can easily be shown that for frequencies well below the cutoff the high-passed output is given by $de_o/dt = 2\pi f_{HP} de_i/dt$ where e_i and e_o are the input and output voltages, and f_{HP} is the -3 dB frequency for the high-pass filter. To minimize the attenuation near the cutoff frequency, the high-pass cutoff frequency was set at 5 – 10 times the frequency of the convected Kolmogorov microscale.

The hot-wire velocity and velocity-derivative signals were digitized using a 15-bit Phoenix A/D converter, so the quantization errors contributed less than 0.01% to the measured

intensities. All data channels were sampled simultaneously at 3 – 5 times the low-pass cutoff frequency discussed above. In order to establish the proper sampling criterion for the moment measurements, the integral time scales were measured at every mesh length along the centerline of the contraction. The integral time scale was obtained using $I = \pi S(0)/2\langle u^2 \rangle$ where $S(0)$ is the zero-frequency asymptote of the half-line spectrum. The effective number of independent realizations was $N = T/(2I)$ where T is the record length. In order to minimize both the quantity of data and the acquisition time while satisfying the statistical convergence criterion, 1024 samples were taken at the optimal rate of $1/4I$. This assured the variability of the mean velocity to be less than 0.4% and that of the mean square fluctuating velocity to be less than about 5%.

IV. Velocity spectra at $x/M = -33$

Figure 4 and 5 show the velocity spectra for the u and v components at $x/M = -33M$ where the turbulence is approximately isotropic. The spectra have been plotted in dimensional logarithmic variables to enable their use as initial conditions in DNS and LES computations. Wavenumber was computed from the frequency by using Taylor's hypothesis. Also shown on the figures are the high and low wavenumber spectral models of George and Gamard[9] computed for the experimental ratio of the longitudinal integral scale to the Kolmogorov microscale of 20. The experimental spectra, F_{11}^1 and F_{22}^1, have been computed in two ways: first directly from the fluctuating velocity components, then by dividing the analog time derivative spectra by frequency squared. The former provides the most accurate values at low wavenumbers, the latter at high (since differentiation effectively boosts the low energy disturbances at high wavenumber). For both approaches, the spectra shown were obtained by subtracting the spectral measurements in the tunnel without grid from those measured with the grid. The reasons for this are described in detail in the next section. The near equality of the spectra measured with both techniques, and their resemblance to the approximate theoretical spectrum, lends considerable credibility, both to the subtraction procedure and the dissipation measurements presented below. The very slight differences occur only in the at the very highest wavenumbers, where the background spectra for the velocity is as large or larger than the turbulence, so the spectra from the derivatives are more accurate.

Figures 6 and 7 show the same data from the figures above plotted in Kolmogorov variables, and presented as linear-linear derivative spectra. For these figures, the velocity spectra were multiplied by frequency squared (or equivalently using Taylor's hypothesis, wavenumber squared). Since at the this location the ratio of wire length to Kolmogorov microscale was approximately five, two theoretical spectra are shown on each plot: one the Gamard/George

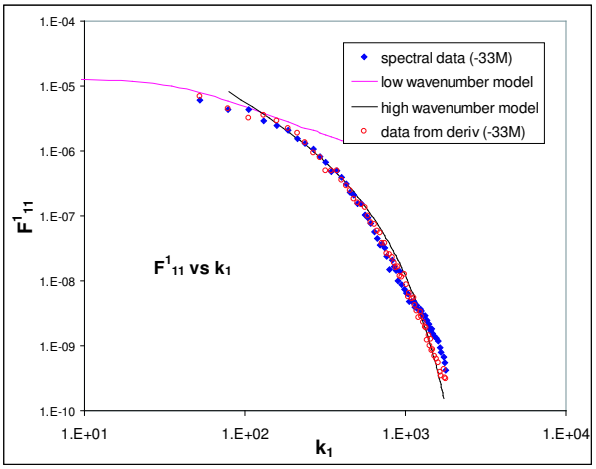

Figure 4. One-dimensional spectrum of u-component of velocity at $x/M = -33$ from contraction exit.

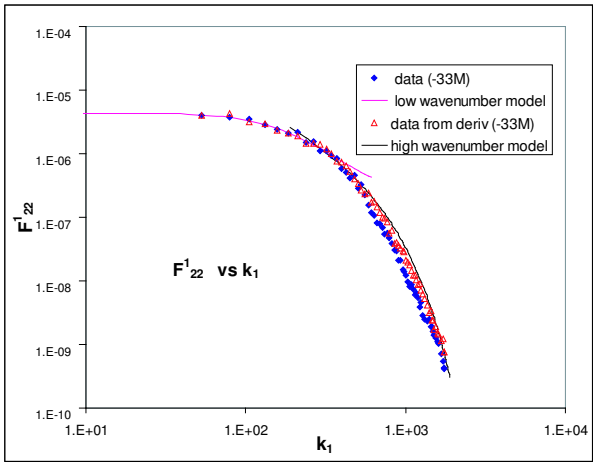

Figure 5. One-dimensional spectrum of v-component of velocity at $x/M = -33$ from contraction exit.

spectrum as above, the other computed from the three-dimensional spectrum by assuming the velocity is 'filtered' or averaged linearly along the wire (i.e., in the manner of Wyngaard,[10] Ewing and George[11]). The 'filtered' u- spectrum resembles very closely the actual data, suggesting the derivative fluctuations may have been underestimated due to wire-roll off by as much as 20% (the difference in the areas under the curves). The v-derivative spectra do not agree as well with the theoretical model, but even so the results are close enough to give confidence in the measurements. It will be concluded below that the measured dissipation turns out to make a negligible contribution to the energy balance throughout most of the contraction. It is clear from the above the this result can not be attributed to the experimental technique, but rather must be a characteristic of the flow.

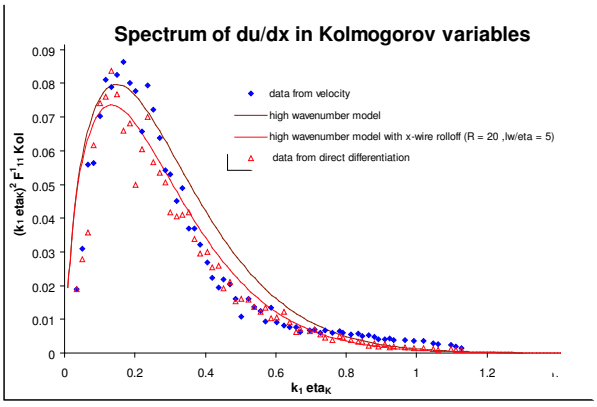

Figure 6. One-dimensional spectrum of u-velocity derivative at $x/M = -33$ in Kolmogorov variables.

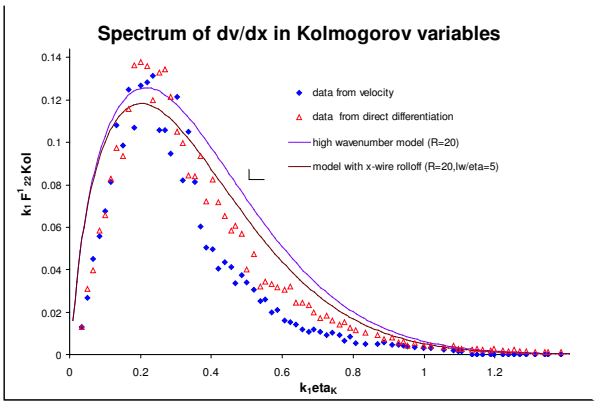

Figure 7. One-dimensional spectrum of v-velocity derivative at $x/M = -33$ in Kolmogorov variables.

V. Background disturbances

Because of the low turbulence intensities, especially through the contraction, it was particularly important to identify all sources of velocity signal contamination, to eliminate them wherever possible, and to establish their statistical correlation with the turbulence when it was not. By using accelerometers and various kinds of mechanical damping, the vibrations of the fan and facility were reduced to levels well below that of the turbulent velocity field. In addition, a number of sources of electronic noise were identified, both within and without the measurement system. These were, for the most part, eliminated by shielding, grounding, and by increasing the gain. These efforts are reported in detail in Han.[12]

In spite of these efforts to reduce both electronic and facility-induced disturbances, non-turbulent flow disturbances which could be ignored in the duct unfortunately dominated the axial component turbulence measurements at the exit of the contraction. This was in part because the axial turbulence component was reduced sharply in the contraction by fact that the 'production' term in the component Reynolds stress equation is negative, and in part because the background flow disturbances were being amplified by the contraction. Figure 8 shows the typical streamwise variation of the rms background disturbances with and without the grid. Clearly the streamwise component is greatly contaminated by the amplification of the background through the contraction, while the radial component is little affected.

Coherence measurements using widely separated hot-wires, with and without the grid present, showed that the frequency of these background disturbances did not change with location in the tunnel or contraction, but their magnitude did as they were amplified in the contraction. The fact that the frequency did not change with the local flow speed made it clear that the origin of the disturbances was not a convected disturbance. Moreover the fact that the coherence was independent of radius without the grid, and nearly identical to the coherence measurements at large separation distances (several turbulence integral scales) with the grid in, suggested strongly that the background disturbances were not correlated at all with the turbulence.

It was possible to confirm that this was indeed the case by summing and differencing the velocity signal from two widely separated wires as shown in Figure 9(left). The details are given in Han,[12] but can be briefly summarized here. Suppose u^t represents the turbulence and $u^{(n)}$ represents the background disturbances. Let $u^{(1)} = u^{(1t)} + u^{(n)}$ and $u^{(2)} = u^{(2t)} + u^{(n)}$ represent the velocity from the two wires at the same axial and radial position but different azimuthal position. The background disturbance have been presumed to be the same for both wires. Because of the azimuthal symmetry, $\langle (u^{(1t)})^2 \rangle = \langle (u^{(2t)})^2 \rangle$. If the wires are

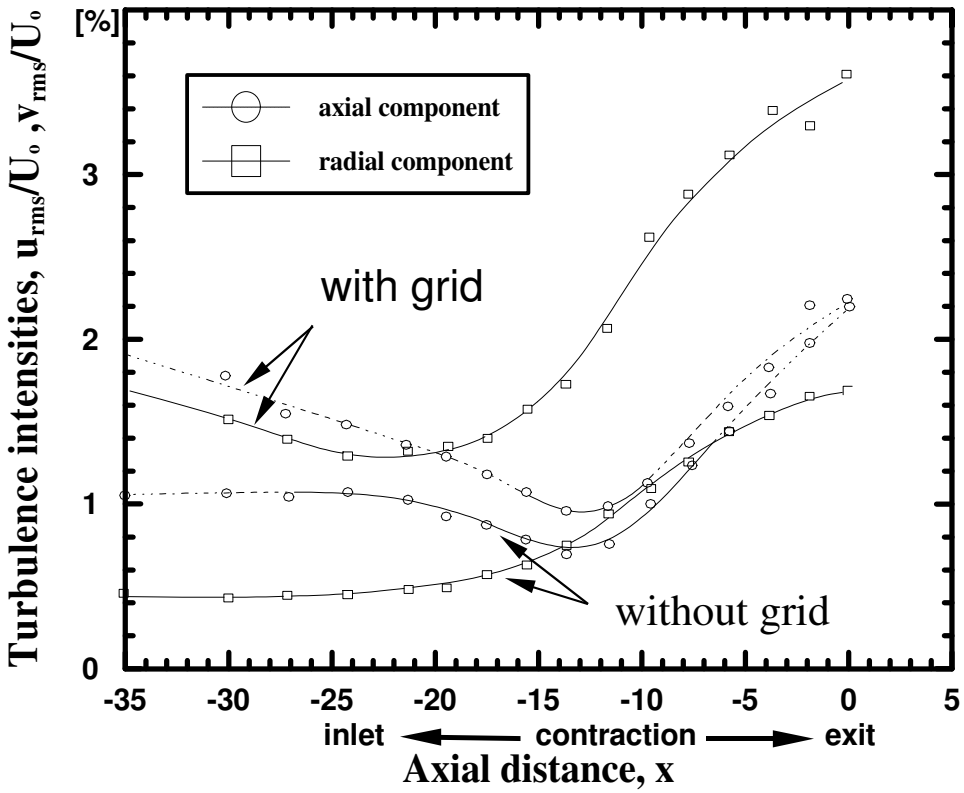

Figure 8. Turbulence intensities with and without grid at 44M (normalized by velocity at grid location).

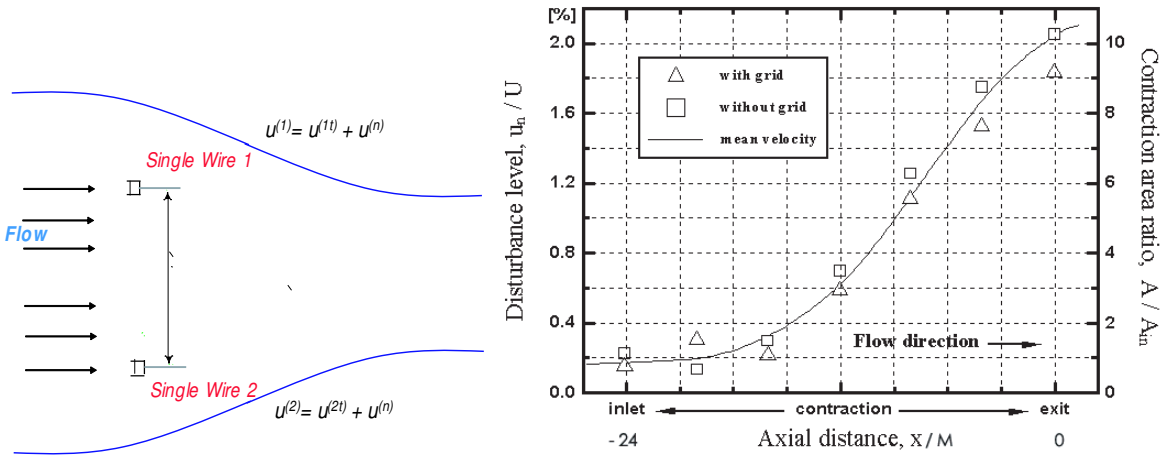

Figure 9. Left: Sketch showing two hot-wires separated enough for turbulence to be uncorrelated. Right: $u^{(n)}/U_o$ as function of distance through contraction plotted together with the centerline mean velocity, U_{cl}/U_o.

widely separated azimuthally so that $\langle u^{(1t)} u^{(2t)} \rangle = 0$, then it is easy to show that

$$4\langle (u^{(n)})^2 \rangle = \langle (u^{(1)} + u^{(2)})^2 \rangle - \langle (u^{(1)} - u^{(2)})^2 \rangle \tag{1}$$

if $u^{(n)}$ and $u^{(t)}$ are uncorrelated. Moreover, the values of $\langle (u^{(n)})^2 \rangle$ so determined should be exactly the same as the values determined in the facility without the grid. The results are shown in Figure 9(right), and to within the experimental error they were.

The streamwise variation of these coherent background disturbances resembles very closely that of the mean velocity (also shown in Figure 9). In particular, it shows approximately the same x-dependence through the contraction, suggesting strongly that the amplification of $u^{(n)}$ is almost entirely due to kinematical considerations, and therefore quite unlike the turbulence. The fact that the background disturbances are spatially coherent across the flow suggests that the walls of the facility can be treated approximately as the surface of either a streamtube or a vortex tube. The streamtube continuity equation for both the mean and fluctuating components is $u \cdot A \approx constant$. A similar relationship applies if the disturbances are rotational since the vortex tube equation is $\omega \cdot A \approx constant$ where ω is the streamwise vorticity component. (Note that equality holds in both these equations only if the profiles are uniform.) Thus if the background fluctuations are either one-dimensional (e.g., acoustical) or in unsteady rigid body rotation (e.g. large scale, but very weak rotational disturbances not removed by the honeycomb), or a combination of both, they are simply amplified by the contraction, exactly as observed. The turbulence, as described below, behaves quite differently since the radial component is amplified while the streamwise component is diminished.

VI. The turbulence intensities

As a consequence of the lack of correlation between the grid-generated and background disturbances, it was possible to directly determine the grid-generated part of the mean square measurements by subtracting the mean square values determined in the facility with no grid from those determined with the grid in. Figures 10, 11, and 12 show the streamwise dependence of the root mean square velocities obtained by subtracting the mean square values without the grid from the mean square value with the grid at 24, 44 and 68 mesh lengths respectively. Now only the radial component increases rapidly in the contraction, but the streamwise component continues to decrease monotonically. As shown in detail in Part 2, this is as expected from the component energy balances since the production term for the streamwise component of the kinetic energy is negative while for the radial component it is positive.

Figure 13 shows the turbulence intensities from the three experimental conditions plotted together. The behavior in the duct clearly depends on the scales and intensities of the turbulence entering the duct. Note that a similar subtraction procedure was used in the grid turbulence measurements of Comte-Bellot and Corrsin,[13] but without the justification

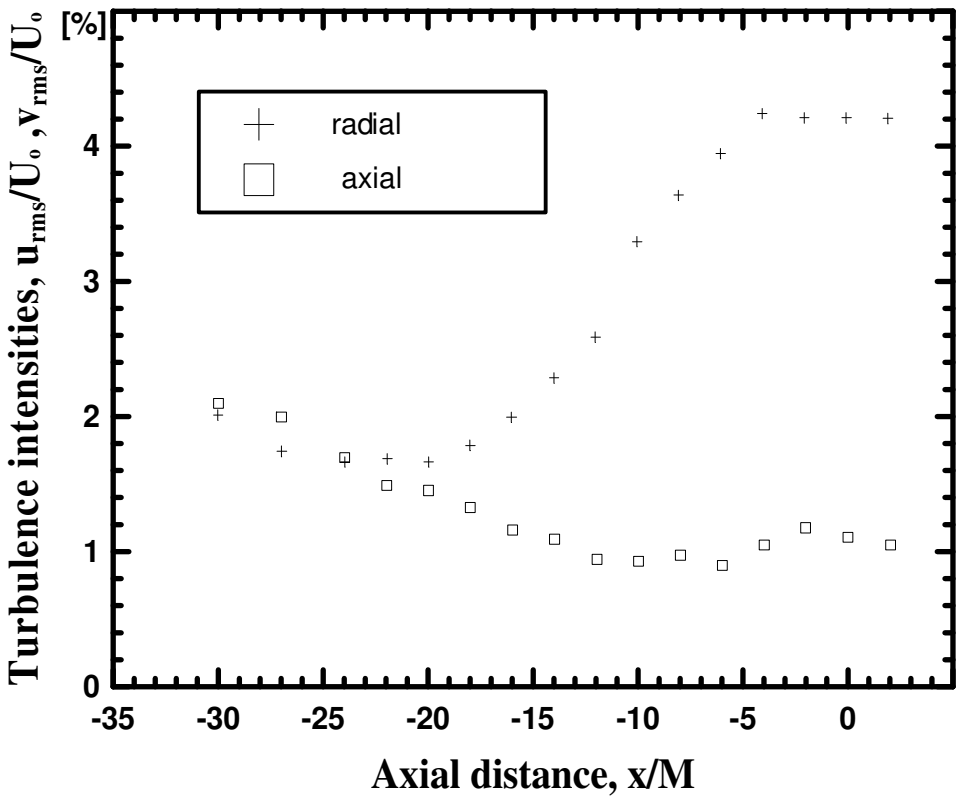

Figure 10. Turbulence intensities with background subtracted. Grid at 24 mesh lengths upstream of contraction exit.

provided here. The absence of such subtraction procedures in the high contraction ratio experiments cited earlier, especially for the streamwise velocity component, is undoubtedly responsible for the anomalous behavior of these data as noted by Shabbir.[5]

VII. The dissipation

The turbulence dissipation rate was also directly estimated using measurements of the mean square fluctuating time derivatives of u and v, together with the quasi-isotropic turbulence estimate of Schedvin et al.:[14]

$$\varepsilon = 3\nu \left[\left(\frac{\partial u}{\partial x} \right)^2 + \left(\frac{\partial v}{\partial x} \right)^2 \right]. \tag{2}$$

The results have been included on the energy balance plots below in Figure 14 and labelled as 'dissipation'. The overall energy balance makes clear that the precise method of estimating the dissipation is almost irrelevant, since in all cases the contribution to the overall energy balance in the contraction was negligible.

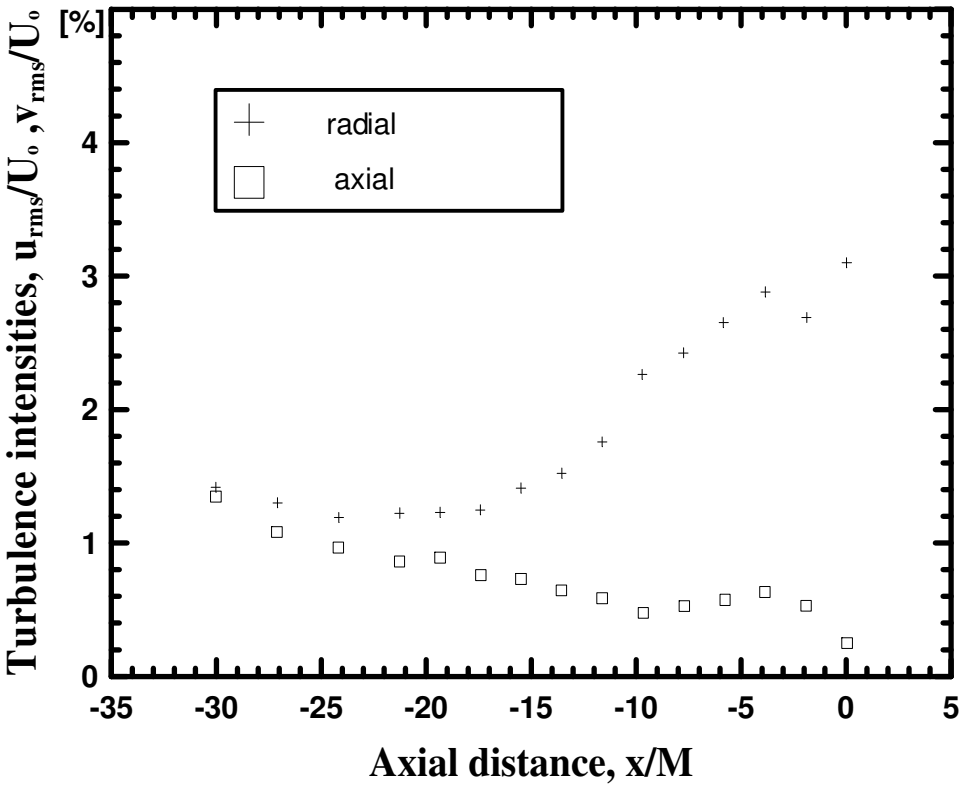

Figure 11. Intensities with background subtracted. Grid at 44 mesh lengths upstream of contraction exit.

VIII. The turbulence energy balances

By assuming the dissipation to be locally homogeneous and using l'Hôpital's theorem and mass conservation, the turbulence kinetic energy (k) equation for an axisymmetric flow along the centerline (see Part II) can be shown to reduce to:

$$U\frac{\partial k}{\partial x} - [\langle u^2\rangle - \langle v^2\rangle]\frac{\partial U}{\partial x} + \varepsilon = -\frac{\partial}{\partial x}[\frac{1}{\rho}\langle pu\rangle + \frac{1}{2}\langle q^2 u\rangle + \nu\frac{\partial k}{\partial x}] + 2\frac{\partial}{\partial r}[\frac{1}{\rho}\langle pv\rangle + \frac{1}{2}\langle q^2 v\rangle + \nu\frac{\partial k}{\partial r}]. \quad (3)$$

The terms on the left-hand-side represent transport by the mean flow, production and dissipation respectively, and the terms on the right-hand-side are the turbulence transport.

From the experimental data it is possible to compute most of the important terms in the kinetic balance of the turbulence: the mean convection, the production, and the dissipation. The remaining terms represent the turbulence transport, which can be estimated together from the remaining balance of the rest.

Figure 14 shows these turbulence energy balances. As noted earlier, the measured dissipation is negligible. Over much of the duct, the kinetic energy balance is almost entirely between the mean convection (or advection) and the production terms, at least until near

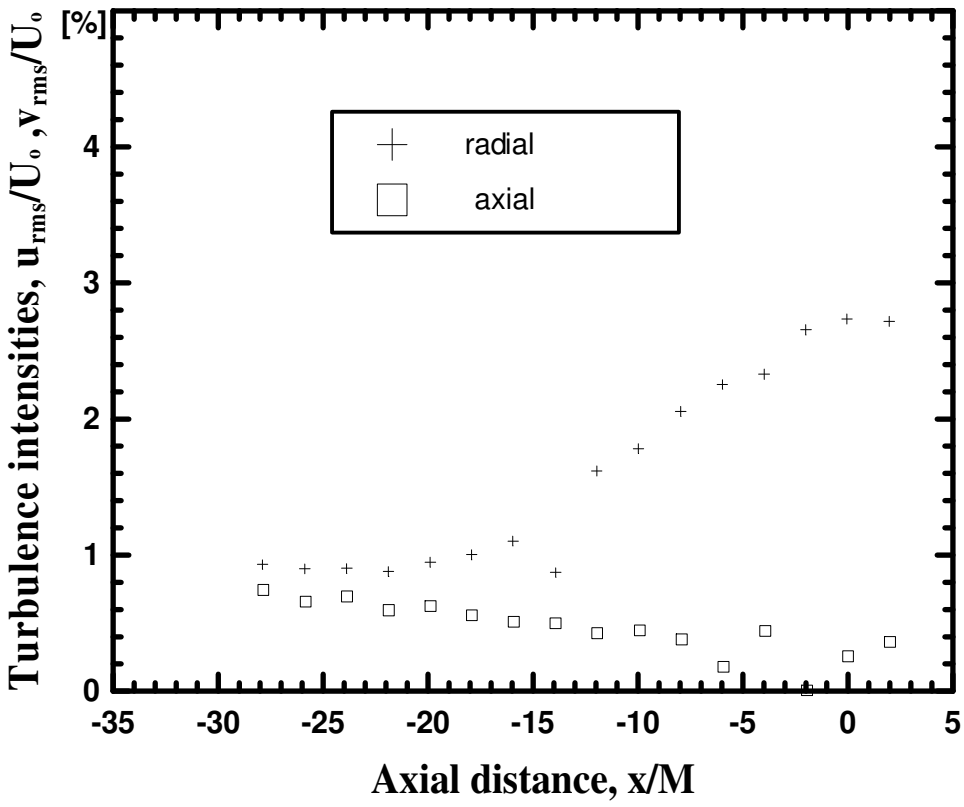

Figure 12. Turbulence intensities with background subtracted. Grid at 68 mesh lengths upstream of contraction exit.

the exit. The turbulent transport terms are more important when the grid is closer to the duct, consistent with the corresponding reduction in the turbulence time scale ratio.

Interestingly, each of the leading terms in the energy balance vanishes identically at some point in the contraction: the mean convection term at the point where the kinetic energy is a minimum, and the production term where $\langle u^2 \rangle = \langle v^2 \rangle$. Since these do not vanish at the same point, there is an extended region where both are small and of the same order as the usually neglected transport terms.

IX. Comparison with the Rapid Distortion Theory

In Part 2 of this paper a new theory of rapid distortion is developed which depended only the neglect of the transport and dissipation terms. Along the centerline of the contraction it was argued that $\langle u^2 \rangle = AU^{-2}$ and $\langle v^2 \rangle = BU$, where A and B are constants for fixed upstream conditions. Figures 15 and 16 show plots of $\langle u^2 \rangle U^2$ and $\langle v^2 \rangle / U$ versus distance through the contraction for the three experiments reported in Part 1. Given the very low turbulence intensities and the consequent difficulty of the experiment, the agreement with the

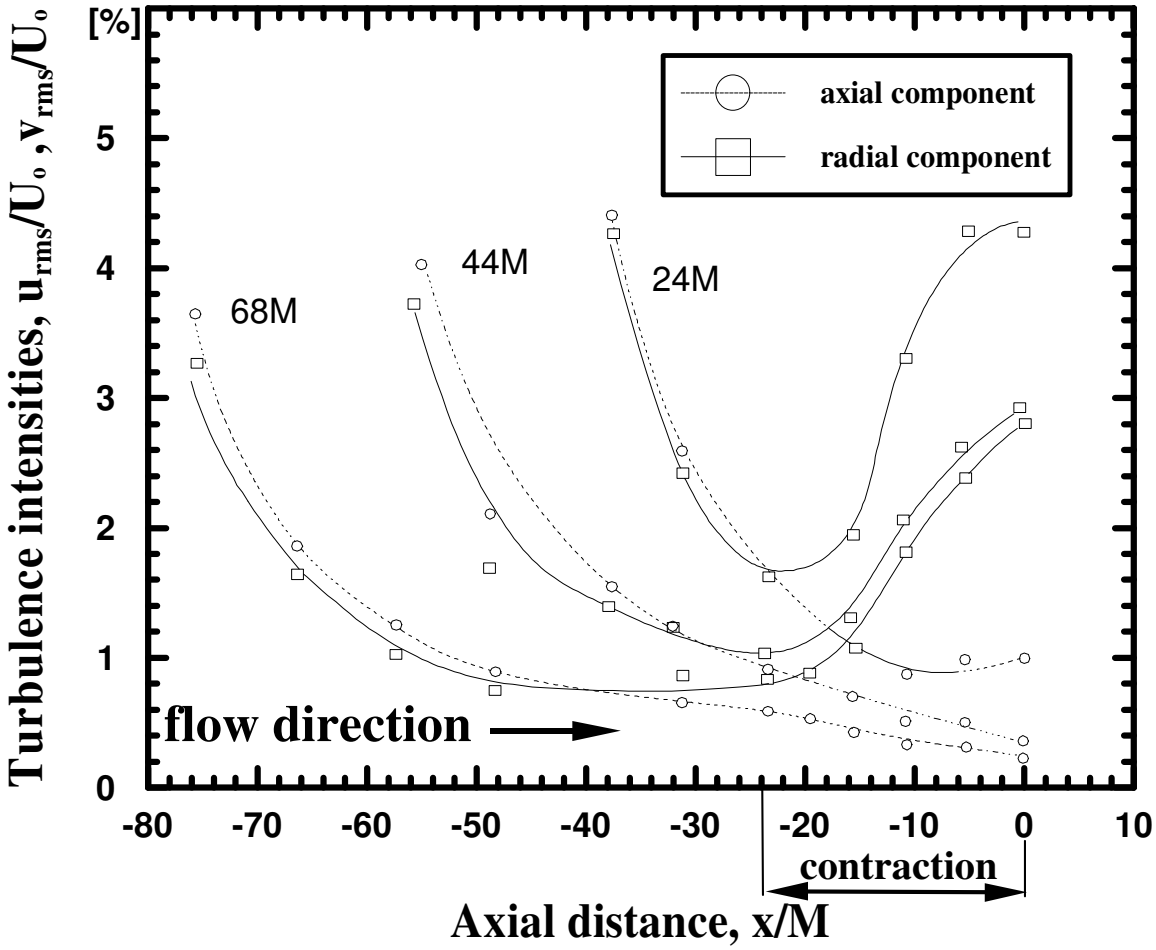

Figure 13. Turbulence intensities with background subtracted for all grid positions plotted together.

new theory is remarkable. The plots for $\langle u^2 \rangle$ are approximately constant until $x/M > -12$, or where the transport terms begin to be important in the kinetic energy balances of figure 14. Moreover, the weaker the transport terms, the closer the data are to the power law behavior. The opposite occurs, however, for $\langle v^2 \rangle$, and the power law solution is valid for the entire duct ($x/M > -24$). This is consistent with the fact that $\langle v^2 \rangle$ increases through the contraction so that its production term increases relative to the neglected transport terms.

X. Summary

An experimental investigation of the kinetic energy balance upstream of and through a strong contraction was carried out in a facility constructed especially for it. The turbulence was generated with a grid in a duct and was nearly isotropic, at least close to the grid. The measurements were performed using hot-wire anemometry. An important aspect of the

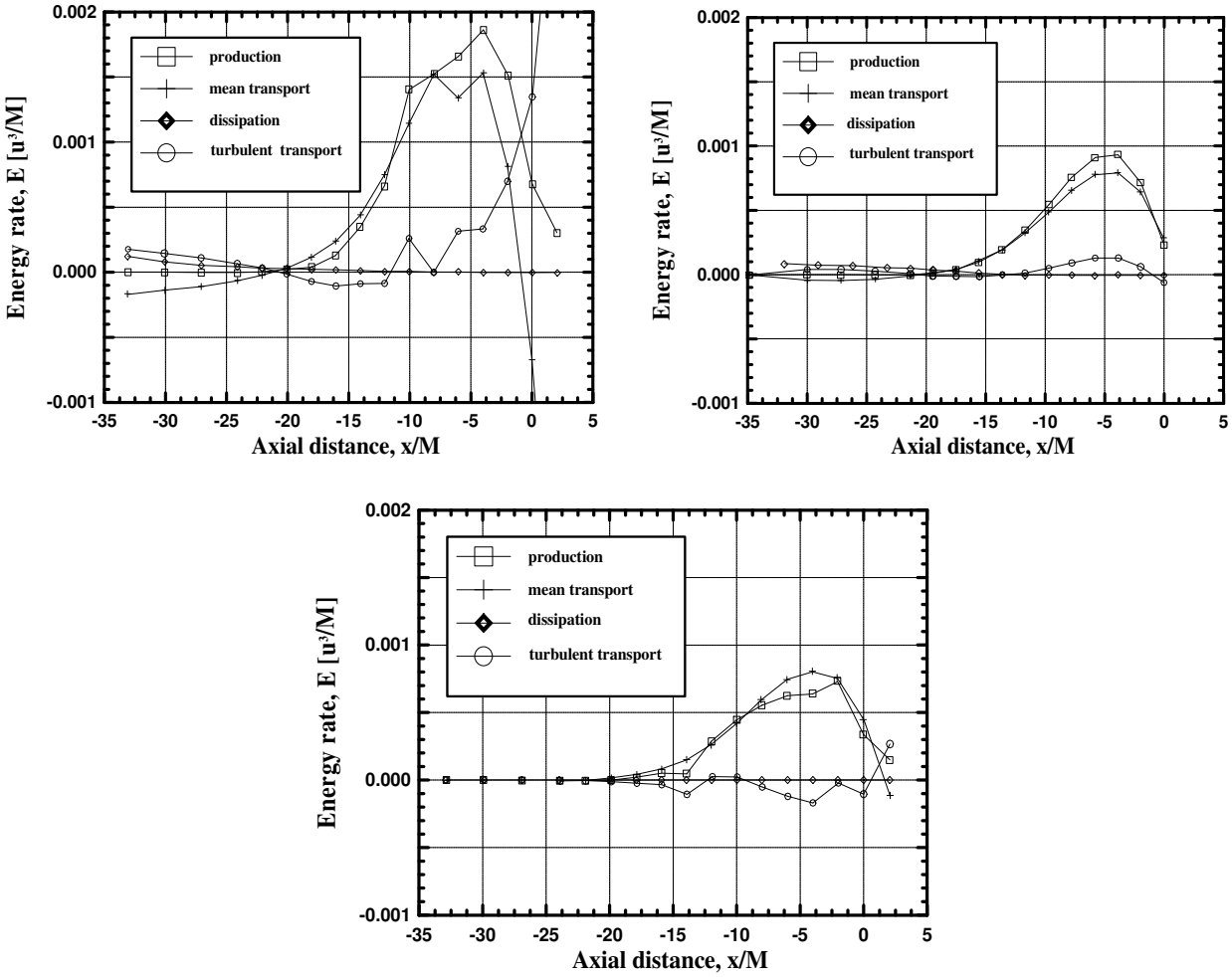

Figure 14. Kinetic energy balance through contraction. Upper left: grid at 24 mesh lengths upstream of contraction entrance. Upper right: grid at 44 mesh lengths. Lower: grid at 68 mesh lengths.

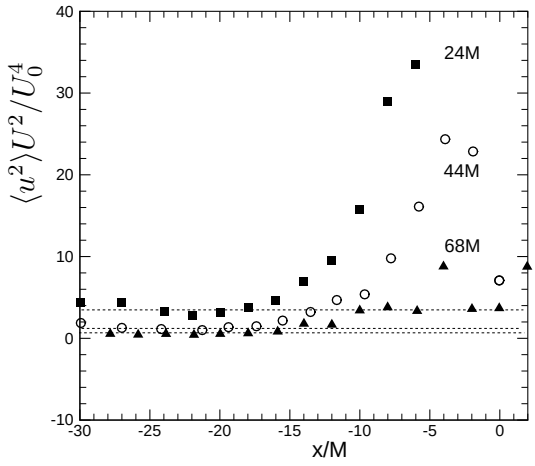

Figure 15. $\langle u^2\rangle$ **times** U^2 **versus** x/M**. 24M, 44M, and 68M represent the different grid positions.**

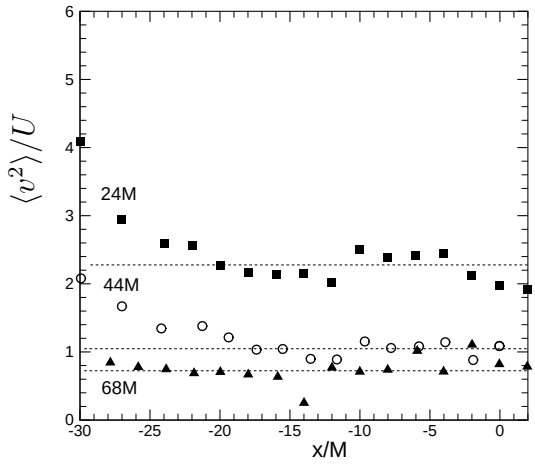

Figure 16. $\langle v^2\rangle$ **divided by** U **versus** x/M**. 24M, 44M, and 68M represent the different grid positions.**

experiment was the manner in which the background disturbances were treated. This was particularly important since these were amplified by the strong contraction. It was possible to show that these disturbances were uncorrelated with the grid-generated turbulence so that they could be removed from the statistics by measuring with and without the grid. This procedure (or rather its absence) largely accounted for the differences from the earlier cited experiments.

By using the corrected intensities it was possible to carry out physically realistic energy balances and identify which terms were important. Another observed effect of the contraction was to influence the apparent turbulence decay rate as far as several diameters upstream of the contraction. This was because even a second-order production term was sufficient to modify the apparent decay rates of the individual components of the turbulence. In fact the production was *negative* for the streamwise component and positive for the radial component. As a consequence, the strong contraction modifies the anisotropy of the turbulence, and is responsible for both the *minimum energy point* and the *crossing point* (where both components are equal). In the vicinity of these points, the leading terms in the kinetic energy balance vanish, and the higher order terms (like the turbulence transport terms) become important in the balance. Finally the results are remarkably consistent with the new rapid distortion theory developed in Part 2 of this paper.

Acknowledgements

The experimental work was initiated while the first two authors were at the State University of New York at Buffalo, and continued with the move of WKG to Chalmers. The authors gratefully acknowledge the contributions of A. Shabbir and D.B. Taulbee who suggested the problem, the technical assistance of S. Woodward, and the many helpful discussions with B.A. Pettersson Reif. This research was carried out with the support of the USA National Science Foundation, Yeungnam University, and Vetenskapsrådet (the Swedish Research Foundation).

References

[1]Ribner, H. and Tucker, M., "Spectrum of Turbulence in a Contracting Stream," Tech. Rep. 1113, NASA Report, 1953.

[2]Uberoi, M. S., "Effect of Wind-tunnel Contraction on Free-stream Turbulence," *J. Aeron. Sci.*, Vol. 23, 1956, pp. 754 – 764.

[3]Ramjee, V. and Hussain, A., "Influence of the Axisymmetric Contraction Ratio on Free-stream Turbulence," *J. Fluids Engr., Trans. ASME*, Vol. 98, No. 3, 1976, pp. 506 – 515.

[4]Tan-atichat, J., *Effects of axisymmetric contractions on turbulence of various scales*, Ph.D. thesis, Illnois Inst. of Tech., Chicago, IL, 1980.

[5]Shabbir, A., *Investigations of the Functional Form of the Coefficients of the Reynolds Stress Closure*, Master's thesis, SUNY/Buffalo, Buffalo, NY, 1983.

[6]Sjögren, T. and Johansson, A. V., "Development and calibration of algebraic nonlinear models for the Reynolds stress transport equations," *Phys. Fluids*, Vol. 12, 2000, pp. 1554 – 1572.

[7]Morell, T., "Comprehensive Design of Axisymmetric Wind Tunnel Contractions." *ASME Trans. Sec. I*, Vol. 97, 1975, pp. 225 – 233.

[8]Han, Y., "Noise Controls in Turbulence Measurements Through a Contraction by Spectral Techniques," *KSME Journal*, Vol. 2, 1988, pp. 140 – 146.

[9]Gamard, S. and George, W., "Reynolds number dependence of energy spectra in the overlap region of isotropic turbulence," *Flow, Turbulence and Combustion*, Vol. 63, 2000, pp. 443–477.

[10]Wyngaard, J., "Measurement of small-scale turbulence with hot-wires," *J. Sci. Instrs.*, Vol. 1, 1968, pp. 1105 – 1108.

[11]Ewing, D., Hussein, H. J., and George, W. K., "Spatial Resolution of Parallel Hot Wire Probes for Derivative Measurements," *J. Exper. Thermal and Fluid Sci.*, Vol. 14, 1996, pp. 42–54.

[12]Han, Y. O., *The Effect of a Contraction on Grid-Generated Turbulence*, Ph.D. thesis, SUNY/Buffalo, Buffalo, NY, 1988.

[13]Comte-Bellot, G. and Corrsin, S., "The Use of a Contraction to Improve the Isotropy of Grid-generated Turbulence," *J. Fluid Mech.*, Vol. 25, 1966, pp. 657–682.

[14]Schedvin, J., Stegun, G., and Gibson, C., "Universal Similarity at High Grid Reynolds Numbers," *J. Fluid Mech.*, Vol. 65, 1974, pp. 561–579.